View metadata, citation and similar papers at core.ac.uk
brought to you by CORE
provided by Online Publishing @ NISCAIR

Indian Journal of Pure & Applied Physics
Vol. 56, May 2018, pp. 399-404

Topas based high birefringent and low loss single mode hybrid-core porous fiber for broadband application

Md Sohidul Islam*, K M Samaun Reza & Mohammad Rakibul Islam
Department of Electrical and Electronics Engineering, Islamic University of Technology, Gazipur 1704, Bangladesh

Received 22 February 2017; accepted 21 August 2017

We present a through numerical analysis of a low loss and highly birefringent hybrid porous core with octagonal cladding structure for terahertz (THz) wave guidance. The proposed photonic crystal fiber (PCF) offers simultaneously low effective material loss (EML) as well as high birefringence in the frequency range of 0.8-1.05 THz with single mode operation. To attain high birefringence we introduce asymmetry in the core using both elliptical and circular air holes (hybrid). The numerical results obtained from the finite element method (FEM) which confirms low EML of 0.044 cm^{-1} as well as a high birefringence of ~0.043 at 0.73 THz operating frequency. Therefore, the fiber is likely to be useful in different THz polarization maintaining applications.

Keywords: Birefringence, Effective material loss, Porous core, Terahertz, Photonic crystal fiber, Wave guide

1 Introduction

Towards achieve the higher channel capacity for guided channel particularly the porous core, photonic crystal fiber for terahertz applications attract much attention to researcher. Terahertz waves (0.1 to 10 THz), share the properties of both of its neighboring bands, millimeter waves and infrared rays in the electromagnetic frequency spectrum. This spectrum has clearly been attracting researchers' interests for the last decades due to its numerous applications in the areas of sensing[1], biotechnology[2], spectroscopy[3], imaging[4-6], and communication[7,8]. One of the most promising applications photonic crystal fiber (PCF) concepts is associated with noninvasive, minimally invasive and intraoperative medical diagnosis. It could be used for noninvasive early diagnosis of skin cancer, minimally invasive diagnosis of colon tissue cancers and intraoperative diagnosis of breast tumors.

Although THz source and detector have been commercialized, the development of the THz waveguide is yet to be commercialized due to the material absorption property of the optical waves in THz region. Wireless transmission requires precision alignment and maintenance, due to the lack of low loss transmission waveguides. Most of the THz system uses free space for its propagation. However the propagation through free space experiences undesirable problems such as tough alignment with additional components, path loss, uncertain absorption loss influenced by the nature of atmosphere and many others.

At the early stages of development, metallic waveguides[9,10], hollow dielectric metal coated tubes were used[11]. The transmission medium showed higher loss and bulky properties. Then the research was shifted from dielectrics to polymers and after that photonic crystal fiber[12,13], hollow core Bragg fiber[14], polymer porous fibers[15], sub-wavelength fibers[16], polystyrene foams[17]and hollow core Bragg fibers[14,18] being introduced subsequently. The micro-structured photonic crystal fiber[19,20] (PCF) with numerous number of air holes in the core and cladding follows the principle of modified total internal reflection (MTIR) or photonic band gap (PBG) effect for light confinement. In the proposed fibre, the light is guided using MTIR as the effective refractive index of the core is higher than that of cladding.

In a porous core octagonal[21] PCF having Topas as the base material for THz wave guidance was proposed. The research showed an EML of 0.076 cm^{-1} but they ignored the analysis of dispersion and core power fraction properties. Later in a porous core fiber[22] having rotated hexagonal structure in core and regular hexagonal structure in cladding was proposed. The research showed a reduced EML of 0.066 cm^{-1} and showed at the power fraction of 40%. However, EML still remained high.

*Corresponding author (E-mail: mdsohidul@gmail.com)

Later, a proposal[23] was made for porous fiber having octagonal structure in both core and cladding. The researchers were able to reduce the EML further to 0.058 cm^{-1}, but they did not mention the dispersion property. Recently, a fiber having circular structure in core and octagonal structure in cladding has been designed[24]. They have showed comparatively lower EML of 0.056 cm^{-1} without testing the single mode properties of the fiber. In recent times, more advanced work has been proposed[25] with circular structure in both core and cladding. They showed a lower EML of 0.053 cm^{-1}. High birefringence can be achieved by either introducing asymmetry to the fiber-core or breaking the symmetry of the fiber cladding. Following this methodology, some remarkable works have been reported to date. For example, in design and fabrication[26] of a porous fiber with rectangular air-holes showed a high birefringence of ~0.012 at 0.65 THz. A squeezed lattice elliptical-hole THz fiber with a birefringence of the order 10^{-2} was proposed in the work[27]. A plastic based[20] PCF showed high birefringence of ~0.021, but the reported propagation loss was very high.

For further improvement, a Topas based porous fiber having hybrid core composed of both elliptical and circular air hole along with unique octagonal cladding structure is presented in this paper. The proposed PCF has shown an extremely lower EML of 0.044 cm^{-1}, birefringence of 0.043 and power fraction of 40.04% at the frequency of 0.73 THz which is better than the other proposed fibers. In our proposed fiber, as transmission of THz waves is based on MTIR, the effects of external environment can totally be neglected. Thus it is expected that the fiber can efficiently be applied for the transmission of broadband THz waves.

2 Geometry of the Proposed Design

Figure 1 depicts (a) cross section of the proposed PCF and (b) enlarged view of the core. In the cladding, the distance between the air holes on two adjacent rings is denoted by Λ and the distance between two adjacent air holes in the same ring is denoted by Λ_1. The relation between them is expressed by Λ_1=0.765Λ. Two-sized air holes of diameter d and $d1$ are used to fill the five layered cladding region. Diameter $d1$ is 0.91 times of d. The core with diameter $D_{core} = 2(\Lambda - d/2)$ is filled with air holes of elliptical and circular shapes. 4 air holes of diameter $d1_c$ have been accumulated in the core. 8 circular air holes of diameter $d2_c$ have been accumulated. 6 circular holes of diameter of $d3_c$ and 4 holes of diameter $d4_c$ have been accumulated with the 4 circular air holes and 15 elliptical air holes in the core. The core diameters $d2_c$, $d3_c$ and $d4_c$ are related to $d1_c$ 0.75 times, 0.1 times and 0.075 times. The length of the major axis of the ellipse is twice that of the diameter of the largest circular core air hole denoted $d1_c$ and the length of the minor axis is equal to $d1_c$. A larger air filling fraction (AFF) 0.76 is used to reduce the EML significantly. A further increase of AFF will result in overlapping of air holes which will make fabrication processes difficult. Thus we have kept AFF value constant at 0.76 for the entire simulation. The size of air holes at the core determines the porosity that can be defined as the ratio of air hole area to the total cross-section area of the core. The air holes in octagonal cladding are 1.32 times larger than the hexagonal core. This results higher confinement of the fiber whereas the effective material loss is

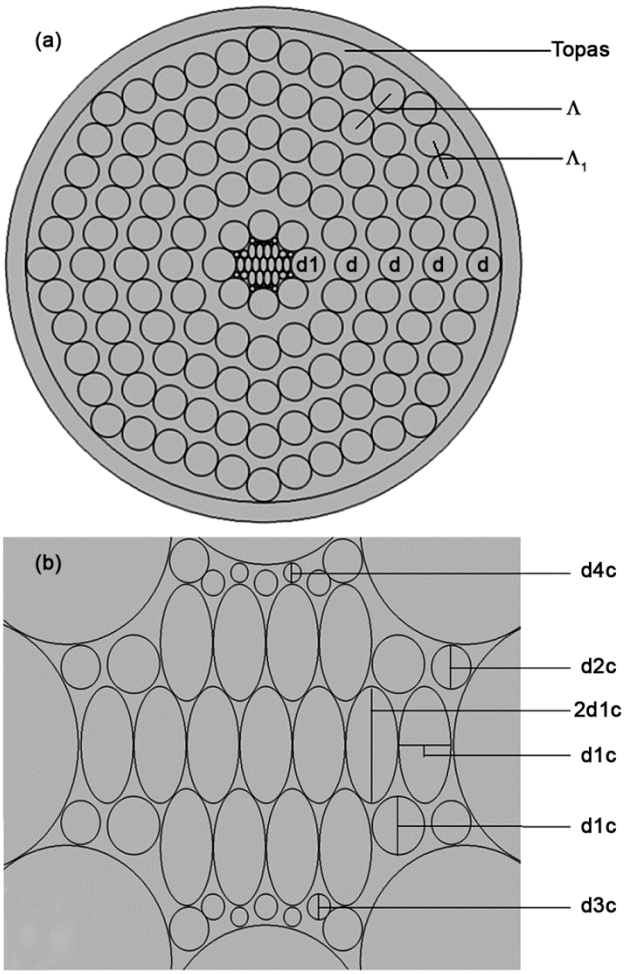

Fig. 1 – (a) Cross section of the proposed PCF and (b) enlarged view of the core.

significantly reduced[28]. Topas is used as the background material for the proposed fiber. The reason for using Topas over other polymer materials includes; lower material absorption loss, constant refractive index n=1.53 in the frequency range[13] of 0.1-1.5 THz. Besides, zero dispersion and humidity insensitivity of Topas facilitates the fiber.

3 Results and Discussion

Finite element modeling (FEM) package, COMSOL v4.2 has been used to simulate and establish the propagation properties of the proposed PCF. Perfectly matched layer (PML) used outside the computational domain is about 9% of the total fiber radius. The power flow distributions at the porosity of 76% at the diameter of 320 µm for both *X* and *Y* polarizations have been showed in Fig. 2. It is observed from Fig. 2 light is well confined in the core for both of the polarization schemes when simulated at 0.73 THz.

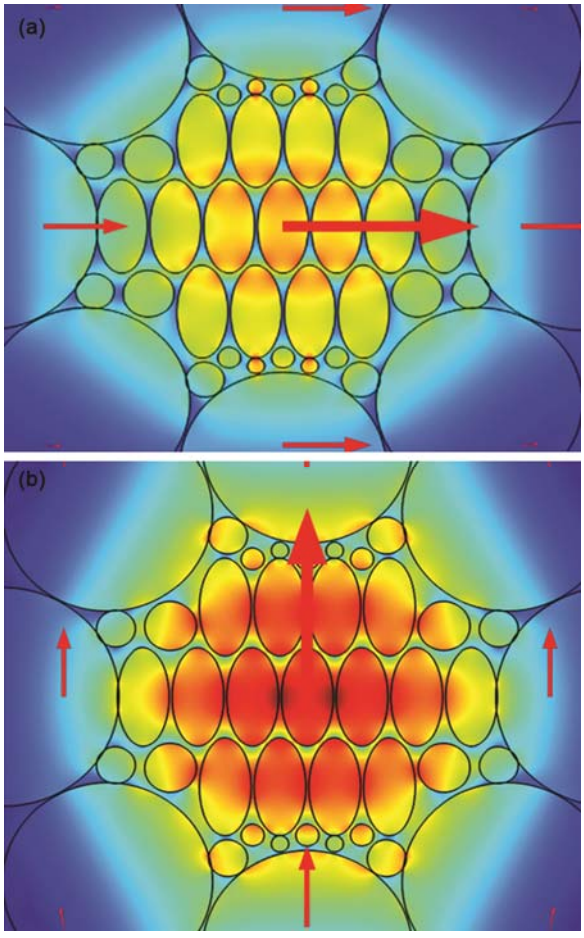

Fig. 2 – Electric field distributions of the proposed PCF at 76% for (a) *X* polarization and (b) *Y* polarization.

In the beginning of simulation, *V*-parameter of the proposed PCF was analyzed to ensure single mode propagation of THz signal. Parameter is calculated by using the following equation[29,30]:

$$V = \frac{2\pi r f}{c}\sqrt{{n_{co}}^2 - {n_{cl}}^2} \leq 2.405 \quad \ldots (1)$$

where r is the core radius, c ($= 3 \times 10^8$ ms^{-1}) is the light speed in vacuum and n_{co} and n_{cl} are the refractive indices of core and cladding respectively. n_{cl} is considered to be 1 because the cladding mainly consists of large number of air holes and the refractive index of air[22] is 1. The core refractive index n_{co} is considered to be effective refractive index (n_{eff}) because of the porous core. To ensure single mode propagation *V*-parameter must be less than or equal to 2.405. For single mode, although launching of optical power into fiber is difficult due to the reduced core radius research suggests the single mode operation for power propagation.

V-parameter as a function of core diameter is shown in Fig. 3. It highlights the fact that for a long range of diameters the proposed PCF shows single mode properties. Best results for birefringence, power flow and EML values were obtained when the proposed fiber was simulated for the diameter of 320 µm at the frequency of 0.73 THz. It is evident from Fig. 3 that the fiber will operate in single mode as the *V*-parameter value at the given diameter is 1.38 which is well below 2.405.

The birefringence which is defined as the absolute value of the differences of n_{eff} between *X* and *Y* polarizations of the proposed PCF is calculated using following equation[31]:

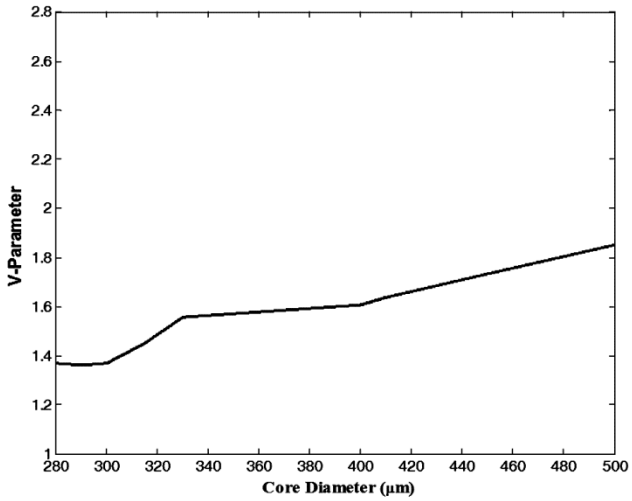

Fig. 3 – *V* parameter versus core diameter at f =0.73 THz and 42% porosity.

$$B = |n_x - n_y| \quad \ldots (2)$$

where n_x and n_y are the refractive indices of two orthogonal components of the polarization maintaining wave. Birefringence as a function of frequency at the porosity of 42% is shown in Fig. 4. It is observed from figures that the birefringence has shown a gradual rise and fall with the variation of frequency within the range of 0.5 to 1.05 THz. The best result of 0.043 was obtained at the frequency of 0.73 THz when the diameter of 320 μm was considered.

Birefringence as a function of D_{core} at different porosities is shown in Fig. 5. It is observed that the reduction in birefringence is due to the increase of porosity. The reason is that at a higher porosity, the mode field is delocalized from the core and spread into the cladding. As a consequence, less power is controlled by the air hole of the core and birefringence is reduced.

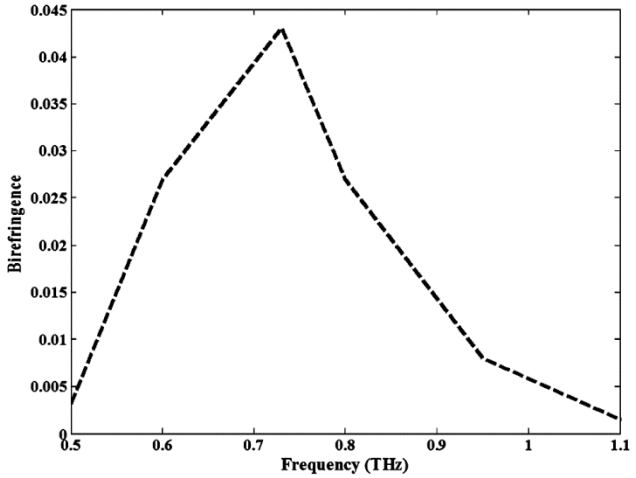

Fig. 4 – Birefringence as a function of frequency at core diameter of 320 μm.

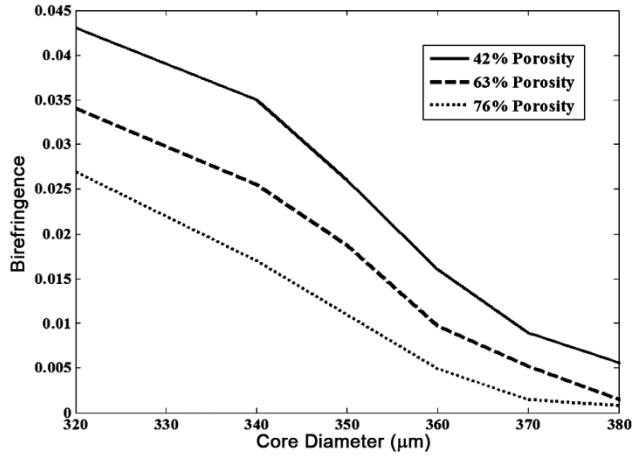

Fig. 5 – Birefringence as a function of core diameter for different porosities at 0.73 THz.

The main concern of the PCF is the reduction of EML, which can be calculated by the following equation[22]:

$$\alpha_{eff} = \sqrt{\frac{\varepsilon_0}{\mu_0}}\left(\frac{\int_{mat} n_{mat}|E|^2 \alpha_{mat}\, dA}{\left|\int_{all} S_z\, dA\right|}\right) \quad \ldots (3)$$

where, ε_0 and μ_0 are the permittivity and the permeability of free space, n_{mat} is the refractive index of the material, α_{mat} is the bulk material absorption loss and S_z is the z component of the poynting vector $S_z^* = ½(E \times H).z$ where E and H are the electric and magnetic field components. The reduction of porosity in the context of increasing the birefringence has resulted in the increase of EML. In Fig. 6, EML for both X and Y polarization at the porosity of 63% and 76% has been showed. The increased porosity of 76% has produced the lowest EML 0.044 cm^{-1} in X-polarization. Increase of diameter increases the EML because the increase of diameter causes the increased scattering of light. In the graph it is observed that EML has increased gradually with the increase of diameter; thus the design has justified the fact.

As the highest birefringence of 0.043 was obtained at the diameter of 320 μm and porosity of 42%, Fig. 7 was generated at a wide range of frequencies to determine the lowest EML at the particular frequency in which the birefringence is the highest. Lowest EML of 0.044 cm^{-1} has been obtained at the frequency of 0.73 THz when the porosity is 42%.

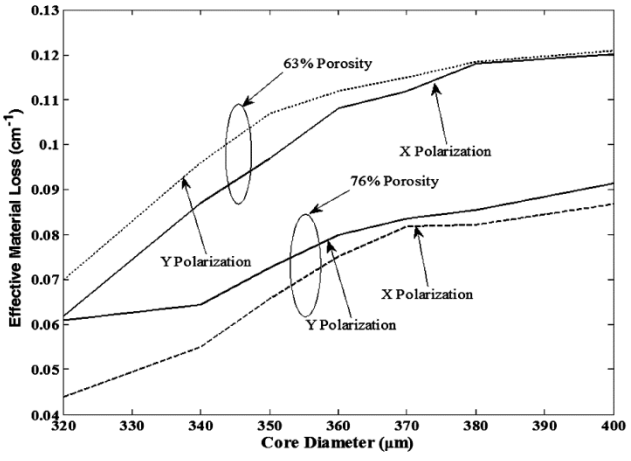

Fig. 6 – EML as a function of core diameters for 63% and 76% porosities at the frequency of 0.73 THz.

Besides EML, another important property called core power fraction can be expressed by the following equation[22]:

$$\eta' = \frac{\int_X S_z dA}{\int_{\text{all}} S_z dA} \quad \ldots (4)$$

where X represents the area covered by the core air holes. As the volume of the core air holes increases with the increase of porosity, power fraction also increases. As noted above, increase of power fraction decreases the birefringence in the proposed model power fraction which was simulated at a lower EML to facilitate the model with increased birefringence.

In Fig. 8, core power fraction at the porosity of 42% and diameter of 320 μm has been plotted against frequencies ranging from 0.5 THz to 1.1 THz. Best result of power fraction for both X polarization and Y polarization was obtained at 0.73 THz which are 41.52% and 39.11%, respectively. Another important parameter which is often considered in PCF designing is confinement loss. It depends upon the core porosity and the number of air holes used in cladding. It can be calculated by taking the imaginary part of the complex refractive index. The confinement loss can be calculated by[22]:

$$L_C = 8.686 \left(\frac{2\pi f}{c}\right) Im\,(n_{\text{eff}}) \left(dB/m\right) \quad \ldots (5)$$

where f is the frequency of the guiding light, c is speed of light in vacuum and $Im(n_{\text{eff}})$ symbolizes the imaginary part of the refractive index.

The confinement loss as a function of frequency is shown in Fig. 9 from where it is observed that as the frequency increases, the confinement loss is scaling down. In the proposed designed fiber, at f =0.73 THz, D_{core}= 320 μm and 42% porosity, a confinement loss of 6.30×10^{-4} cm^{-1} is obtained which is negligible compared to the calculated EML. Table 1 shows the comparison of effective material loss and

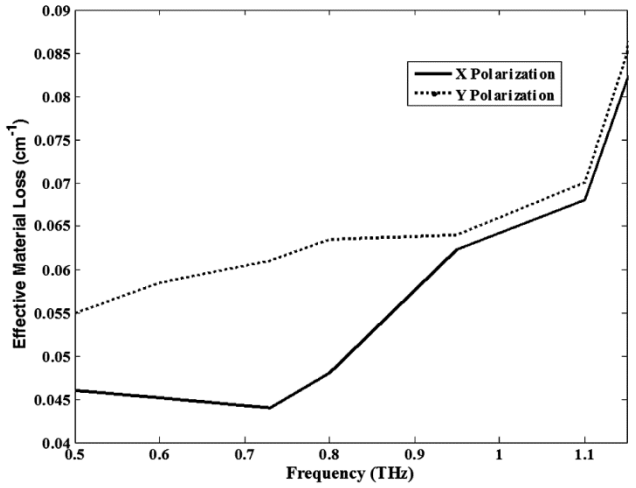

Fig. 7 – EML as a function of frequency at 320μm with the porosity 42%.

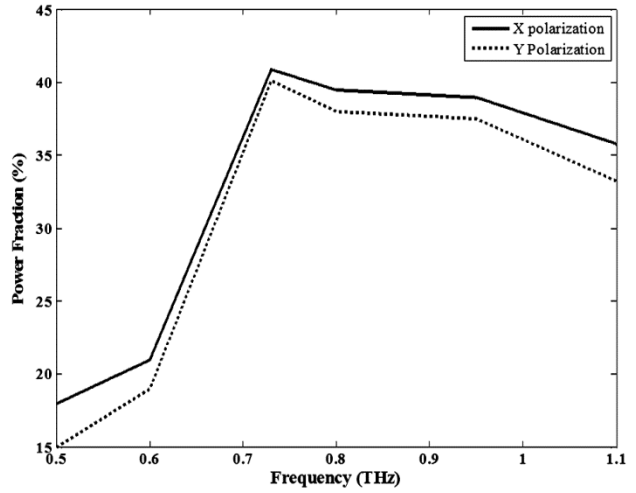

Fig. 8 – Core power fraction at different frequencies at the porosity of 42% and at core diameter of 320 μm.

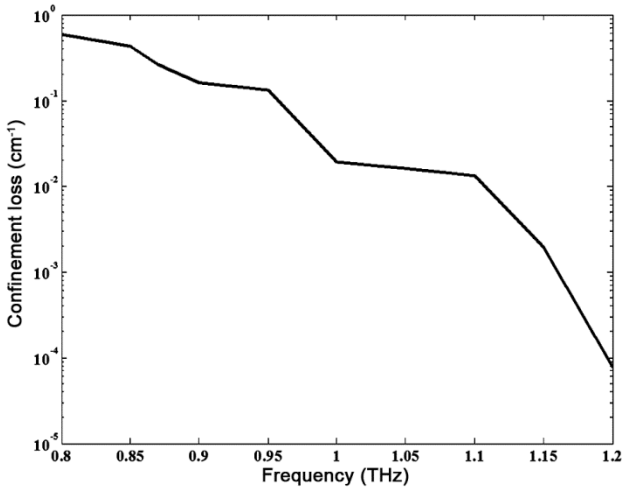

Fig. 9 – Confinement loss as a function of frequency at 320 μm with the porosity of 42%.

Table 1 – The comparison of effective material loss and birefringence of our proposed PCF with other design in the literature.

Literature	EML (cm^{-1})	Birefringence
Hasan *et al.*[37]	0.085	0.0483
Islam *et al.*[38]	0.070	0.018
Islam *et al.*[39]	0.100	Not mentioned
Islam *et al.*[40]	0.066	Not mentioned
Revathi *et al.*[41]	Not mentioned	0.034
Present work	0.044	0.043

birefringence of our proposed PCF with other design in the literature.

Finally, we explored the fabrication possibility of our proposed design. The proposed PCF core contains air holes with different dimensions. The fabrication of PCF will be challenging. As technology is developing every day, the challenge of designing the PCF is accordingly realized. The capillary stacking[32,33] and sol-gel[33-36] techniques are the best choice to fabricate where the dimensions of the proposed PCF can be adjusted freely.

4 Conclusions

A new PCF with hybrid core is being proposed which is important for polarization maintaining applications in the THz regime. It has been shown that asymmetry of air holes in the fiber core leads to low EML of 0.044 cm^{-1} and high birefringence of ~0.043. The proposed design is expected to be fabricated using the concurrent fabrication technology combining the capillary stacking and sol-gel techniques. Therefore, the proposed design may be the potential candidate for higher channel capacity network, coherent communication and sensing application in THz regime.

References

1 Jacobsen R H, Mittleman D M & Nuss M C, *Opt Lett*, 21 (1996) 2011.
2 Nagel M, Bolivar P H, Brucherseifer M & Kurz H, *Appl Phys Lett*, 80 (2002) 154.
3 Zhang J Q & Grischkowsky D, *Opt Lett*, 29 (2004) 1617.
4 Chan W L, Deibel J & Mittleman D M, *Rep Progr Phys*, 70 (2007) 1325.
5 Mittleman D M, Gupta M, Neelamani R, Baraniuk R G, Rudd J V & Koch M, *Appl Phys B*, 68 (1999) 1085.
6 Chen H T, Padilla W J, Cich M J, Azad A K, Averitt R D & Taylor A J, *Appl Phys Lett*, 83 (2003) 3009.
7 Moller L, Federici J, Sinyukov A, Xie C, Lim H C & Giles R C, *Opt Lett*, 33 (2008) 393.
8 Ung B, Mazhorova A, Dupuis A, Rozé M & Skorobogatiy M, *Opt Exp*, 19 (2011) B848.
9 Wang K & Mittleman D M, *Nature*, 432 (2004) 376.
10 Gallot G, Jamison S P, McGowan R W & Grischkowsky D, *J Opt Soc Amer B*, 17 (2000) 851.
11 Bowden, B, Harrington J A & Mitrofanov O, *Opt Lett*, 32 (2007) 2945.
12 Ghasemi A H & Latifi H, *Opt Lett*, 37 (2012) 2727.
13 Nielsen K, Rasmussen H K, Aurèle J L, Paul A, Planken C M, Bang O & Jepsen P U, *Opt Exp*, 17 (2009) 8592.
14 Skorobogatiy M & Dupuis A, *Appl Phys Lett*, 90 (2007) 113514.
15 Atakaramians S, Shahraam A V, Fischer B M, Abbott D & Monro T M, *Opt Exp*, 16 (2008) 8845.
16 Chen L J, Chen H W, Kao T F, Lu J Y & Sun C K, *Opt Lett*, 31 (2006) 308.
17 Zhao G, Mors M, Wenckebach T, Paul A & Planken C M, *J Opt Soc Amer B*, 19 (2002) 1476.
18 Lu J Y, Yu C P, Chang H C, Chen H W & Li Y T, *Appl Phys Lett*, 92 (2008) 064105.
19 Hameed M F O, Heikal A M, Younis B M, Abdelrazzak M & Obayya S S A, *IEEE Photonics J*, 1 (2009) 265.
20 Hameed M F O & Obayya S S A, *IEEE J Lightwave Technol*, 30 (2012) 96.
21 Kaijage S F, Ouyang Z & Jim X, *IEEE Photon Technol Lett*, 25 (2013) 1454.
22 Islam R, *Opt Fiber Technol*, 24 (2015) 38.
23 Rana S, Hasanuzzaman G K M, Habib S, Kaijage S F & Islam R, *Opt Eng*, 53 (2014) 115.
24 Hasan M I, Abdurrazzak S M, Hasanuzzaman G K M & Habib M S, *IEEE Photon Technol Lett*, 26 (2014) 2372.
25 Islam R & Rana S, *Opt Eng*, 54 (2015) 95.
26 Emiliyanov G, Jensen J B, Bang O & Hoiby P E, *Opt Lett*, 32 (2007) 460.
27 Nielsen K, Rasmussen H K, Jepsen P U & Bang O, *Opt Lett*, 36 (2011) 666.
28 Kaneshima K, Namihira Y, Zou Nianyu, Higa Hiroki & Nagata Y, *IEICE Trans Electron*, E89-C (2006) 830.
29 Snyder AW, *Optical waveguide theory*, (Chapman & Hall: London, UK), 1983.
30 Bao H, Nielsen K, Rasmussen H K & Jepsen P U, *Opt Exp*, 20 (2012) 29507.
31 Chen N, Liang J & Ren L, *Appl Opt*, 52 (2013) 5297.
32 Liang J, Ren L, Chen N & Zhou C, *Opt Commun*, 295 (2013) 257.
33 Hasan M I, Habib M S, Habib M S & Razzak S M A, *Opt Fiber Technol*, 20 (2014) 32.
34 Roze M, Ung B, Mazhorova A & Walther M, *Opt Exp*, 19 (2011) 9127.
35 Hasan M I, Habib M S & Habib M S, *Photon Nanostruct Fundam Appl*, 12 (2014) 205.
36 Bise R T & Trevor D J, *Optical fiber communication conference*, 2005.
37 Hasan M R, Anower M S, Islam M A & Razzak S M A, *Appl Opt*, 55 (2015) 4145.
38 Islam R, Habib M S, Hasanuzzaman G K M, Rana S, Sadath M A & Markos C, *IEEE Photon Technol Lett*, 28 (2016) 1537.
39 Islam R, Rana S, Ahmad R & Kaijage S F, *IEEE Photon Technol Lett*, 27 (2015) 2242.
40 Islam R, Hasanuzzaman G K M, Habib M S, Rana S & Khan M A G, *Opt Fiber Technol*, 24 (2015) 38.
41 Revathi S, Inabathini S & Sandeep R, *Opt Appl*, 45 (2015) 15.